International Journal of Advanced Biochemistry Research

ISSN Print: 2617-4693
ISSN Online: 2617-4707
NAAS Rating (2026): 5.29
IJABR 2026; SP-10(8): 2463-2473
www.biochemjournal.com
Received: 04-07-2026
Accepted: 10-08-2026

Surumi Noorudeen
Trainee at Bioinformatics Project and Research Institute, Noida, Uttar Pradesh, India

Uma Kumari
Senior Bioinformatics Scientist, Bioinformatics Project and Research Institute, Noida, Uttar Pradesh, India

Corresponding Author:
Uma Kumari
Senior Bioinformatics Scientist, Bioinformatics Project and Research Institute, Noida, Uttar Pradesh, India

Structure-based design of DYRK1A inhibitors for Alzheimer's disease

Surumi Noorudeen and Uma Kumari

DOI: https://www.doi.org/10.33545/26174693.2026.v10.i8Sab.9770

Abstract
Alzheimer's disease (AD) is the leading cause of dementia and remains without a disease-modifying cure, in part because most approved therapies target symptoms rather than the underlying molecular drivers of neurodegeneration. Dual-specificity tyrosine phosphorylation-regulated kinase 1A (DYRK1A) has emerged as a mechanistically attractive target because it phosphorylates tau at pathological residues and modulates amyloid precursor protein processing, placing it upstream of both hallmark AD pathologies. This study combined sequence-level bioinformatics with structure-based drug design to evaluate the human DYRK1A kinase domain (PDB ID: 7O7K) as a template for inhibitor discovery. BLASTP and phylogenetic analysis confirmed the identity and evolutionary conservation of the retrieved sequence, while ERRAT (quality factor 96.37%) and Ramachandran plot analysis (88.7% of residues in the most favoured region, no residues in disallowed regions) established that the structure was of sufficient stereochemical quality for downstream docking. Protein-protein interaction mapping using STRING placed DYRK1A within a ten-partner interaction hub linked to DNA-damage repair, calcineurin-NFAT signalling, and transcriptional regulation, and cross-referencing this network against the KEGG Alzheimer's disease pathway (hsa05010) supported its disease relevance. Blind docking of five candidate ligands, pazopanib, kaempferol, emodin, sunitinib, and the co-crystallized reference inhibitor abemaciclib, against the validated receptor using CB-Dock and AutoDock Vina identified pazopanib as the strongest predicted binder of the DYRK1A ATP-binding cleft (Vina score −10.3 kcal/mol, cavity volume 5685 Å³), with abemaciclib a close second (−10.7 kcal/mol at a smaller cavity) and the remaining three ligands showing consistent, overlapping engagement of the same pocket. These findings support DYRK1A as a structurally and biologically validated target and nominate pazopanib as a candidate for further ADMET profiling and molecular dynamics evaluation as part of a drug-repurposing strategy against Alzheimer's disease.

Keywords: DYRK1A, Alzheimer's disease, molecular docking, structure-based drug design, CB-Dock, protein-protein interaction network

1. Introduction

Alzheimer's disease (AD) is the most common neurodegenerative disorder and accounts for 60-70% of all dementia cases worldwide, producing progressive decline in memory, cognition, and the capacity for independent living [1, 2]. Despite decades of research, treatment remains largely symptomatic, and a mechanistic understanding of the pathways driving neurodegeneration is essential for developing disease-modifying therapies [1, 2, 3].

AD pathology is defined by extracellular amyloid-β (Aβ) plaques, intracellular neurofibrillary tangles composed of hyperphosphorylated tau, synaptic dysfunction, chronic neuroinflammation, and progressive neuronal loss [2, 4, 5]. Abnormal tau phosphorylation in particular drives tau misfolding and tangle formation, which has focused considerable research attention on the kinases responsible for this hyperphosphorylation [4, 5, 6]. Among these kinases, dual-specificity tyrosine phosphorylation-regulated kinase 1A (DYRK1A) has emerged as one of the most promising targets for AD therapy [7, 8]. Encoded on chromosome 21q22.13 and belonging to the CMGC family of protein kinases, DYRK1A normally supports neuronal differentiation, synaptic plasticity, and brain development, but its dysregulation is implicated in Alzheimer's disease, Down syndrome, and Parkinson's disease [7, 9, 10]. Experimentally, DYRK1A phosphorylates tau at several pathological residues and separately promotes amyloid precursor protein processing and Aβ production, placing it upstream of both major pathological arms of AD and making it an attractive target for disease-modifying, rather than purely symptomatic, intervention [6, 7, 10].

Structure-based drug design (SBDD) has become central to modern kinase-inhibitor discovery, using high-resolution three-dimensional protein structures to predict protein-ligand interactions computationally prior to experimental testing [11, 12]. The present study uses the crystal structure of the human DYRK1A kinase domain (PDB ID: 7O7K), solved at 1.82 Å resolution in complex with the FDA-approved CDK4/6 inhibitor abemaciclib, which also inhibits DYRK1A [8]. This co-crystal structure defines the ATP-binding pocket and the residues governing ligand recognition, providing an experimentally validated template for docking, virtual screening, and inhibitor optimization [8, 11, 12]. Reported DYRK1A inhibitors, including harmine derivatives, leucettines, INDY-class compounds, and repurposed kinase inhibitors such as abemaciclib, continue to face limitations in selectivity, pharmacokinetics, blood-brain barrier permeability, and off-target toxicity [13], and recent computational screening studies have continued to identify new candidate chemotypes with improved properties [13, 14]. In parallel, next-generation sequencing (NGS) has transformed the genetic characterization of complex diseases such as AD, enabling rapid, massively parallel identification of causal and risk-associated variants. NGS-based studies have identified causal genes (APP, PSEN1, PSEN2) and risk loci (APOE, TREM2, SORL1, BIN1, CLU, PICALM) through genome-wide association studies, and transcriptomic profiling has clarified dysregulated pathways in neuroinflammation, synaptic dysfunction, and oxidative stress [15-20]. Integrating this genomic evidence with structural biology allows disease-relevant targets to be prioritized on the basis of both genetic and structural evidence, a systems-level strategy that improves on treating sequence and structure as independent lines of investigation [17, 18, 11, 21].Most published DYRK1A studies, however, have applied computational screening or genomic analysis separately rather than in combination [17, 11]. The present study therefore integrates NGS-informed sequence analysis with structure-based drug design targeting human DYRK1A (PDB ID: 7O7K), combining protein sequence validation, structural quality assessment, protein-protein interaction network analysis, and molecular docking of candidate ligands, with the goal of identifying and structurally justifying candidate inhibitors for further development against Alzheimer's disease [11, 17, 21].

2. Materials and Methods

This study followed an integrated computational workflow comprising protein structure retrieval and validation, sequence similarity and phylogenetic analysis, protein-protein interaction network mapping, and structure-based molecular docking, summarized in the sub-sections below [22-25].

2.1 Retrieval of the DYRK1A Protein Structure and Sequence

The three-dimensional crystal structure of human DYRK1A was retrieved from the Protein Data Bank (PDB ID: 7O7K), corresponding to the DYRK1A kinase domain co-crystallized with abemaciclib [22, 23, 26], and downloaded in .pdb format. The corresponding amino-acid sequence was obtained in FASTA format from the NCBI Molecular Modelling Database (MMDB), which links structural, sequence, and conserved-domain annotations to each PDB entry [24, 27].

2.2 Sequence Similarity and Phylogenetic Analysis

The retrieved FASTA sequence was submitted as a query to BLASTP (Basic Local Alignment Search Tool for Proteins) against the PDB protein database using default parameters [28, 29]. Homologous sequences were evaluated by maximum score, query coverage, E-value, and percentage identity [29, 30]. Evolutionary relationships among the resulting homologues were then visualized using the BLAST Distance Tree Viewer, which applies the Fast Minimum Evolution algorithm to cluster sequences by evolutionary distance [31].

2.3 Protein Structure Validation

Structural quality was assessed using the SAVES v6.0 server [32]. ERRAT was used to evaluate overall model quality from the statistics of non-bonded atomic interactions, with structures classified as excellent (≥95%), acceptable (80-90%), or requiring refinement (<80%) **[33, 34]**. Stereochemical quality was separately assessed using PROCHECK, which generates a Ramachandran plot showing the distribution of backbone dihedral (φ/ψ) angles across the most favoured, additionally allowed, generously allowed, and disallowed regions [34].

2.4 Structure Visualization, Ligand Contacts, and B-Factor Analysis

The validated DYRK1A structure was visualized in PyMOL (Version 3.0, Schrödinger, LLC) [35, 36] with a white background and water molecules removed. The co-crystallized ligand was highlighted and its surrounding pocket rendered as a molecular surface, with contact residues labelled using PyMOL's residue annotation tools. Hydrogen bonds and interatomic distances were measured using PyMOL's built-in distance tools. Per-residue B-factors were extracted and mapped onto the structure to identify conformationally flexible, solvent-exposed regions relative to the stable protein core [35, 37].

2.5 Molecular Docking

Molecular docking was performed using a curvature-based blind-docking server that automatically detects candidate binding cavities on the protein surface using its CurPocket algorithm and docks ligands into each predicted cavity with AutoDock Vina (version 1.1.2), without requiring a predefined grid box [42, 43, 44]. The validated receptor (PDB ID: 7O7K) was uploaded in PDB format. Structure data files (SDF) for five candidate ligands, pazopanib (PubChem CID 10113978), kaempferol (PubChem CID 5280863), emodin (PubChem CID 3220), sunitinib (PubChem CID 5329102), and abemaciclib (PubChem CID 46220502), were retrieved from PubChem [45] and docked individually. For each ligand, CB-Dock ranked the predicted cavities by AutoDock Vina score (kcal/mol), with more negative scores indicating more favourable predicted binding, alongside cavity volume ($Å^3$) and docking-box dimensions. The top-ranked cavity for each ligand was carried forward for detailed contact-residue analysis in PyMOL [35, 36]. Abemaciclib, the ligand co-crystallized with PDB ID: 7O7K, was re-docked using the same protocol as an internal positive control.

2.6 Protein-Protein Interaction and Pathway Analysis

A protein-protein interaction (PPI) network for DYRK1A was constructed using STRING (Search Tool for the

Retrieval of Interacting Genes/Proteins, version 12.0) [38], querying the DYRK1A gene symbol against the Homo sapiens genome at the default medium-confidence threshold. Predicted partners were ranked by the STRING combined confidence score, which integrates experimental, curated-database, co-expression, genomic-context, and text-mining evidence. To place this network in a disease context, the DYRK1A interaction partners identified by STRING were cross-referenced against the KEGG Alzheimer's disease pathway (map hsa05010) [50, 51], which curates the amyloidogenic, tau-hyperphosphorylation, and neuroinflammatory processes underlying AD pathology.

3. Results

3.1 Retrieval and Overview of the DYRK1A Structure

The crystal structure of human DYRK1A (PDB ID: 7O7K) was successfully retrieved from the Protein Data Bank. The deposited structure represents the kinase domain co-crystallized with abemaciclib and belongs to the transferase class, with Chain A containing the complete kinase domain used as the query for downstream sequence and structural analyses (Figure 1). [52, 53]

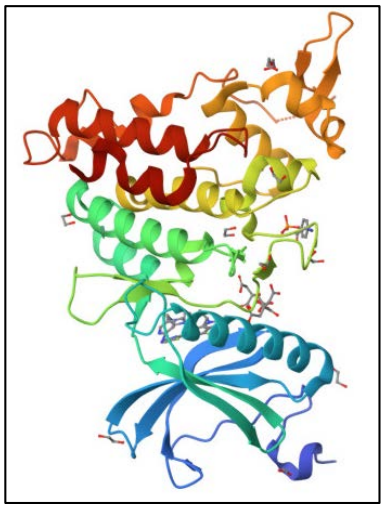

Fig 1: Crystal structure of the human DYRK1A kinase domain (PDB ID: 7O7K) retrieved from the Protein Data Bank.

3.2 Sequence Similarity Analysis

BLASTP analysis confidently identified the query sequence as human DYRK1A. All significant alignments returned an E-value of 0.0, query coverage of 99-100%, and sequence identity of 99.72-100% against previously deposited human and mouse DYRK1A structures (Figure 2), confirming the identity of the retrieved protein and its suitability for downstream structural analysis [54, 55].

3.3 Phylogenetic Analysis

The BLAST Distance Tree Viewer placed the query protein within the CDC-like kinase (CLK)/DYRK kinase family, clustering closely with other human DYRK and CLK isoforms (Figure 3). This pattern is consistent with the established classification of DYRK1A within the CMGC group of the human kinome and confirms strong evolutionary conservation of the kinase domain used as the docking template [56].

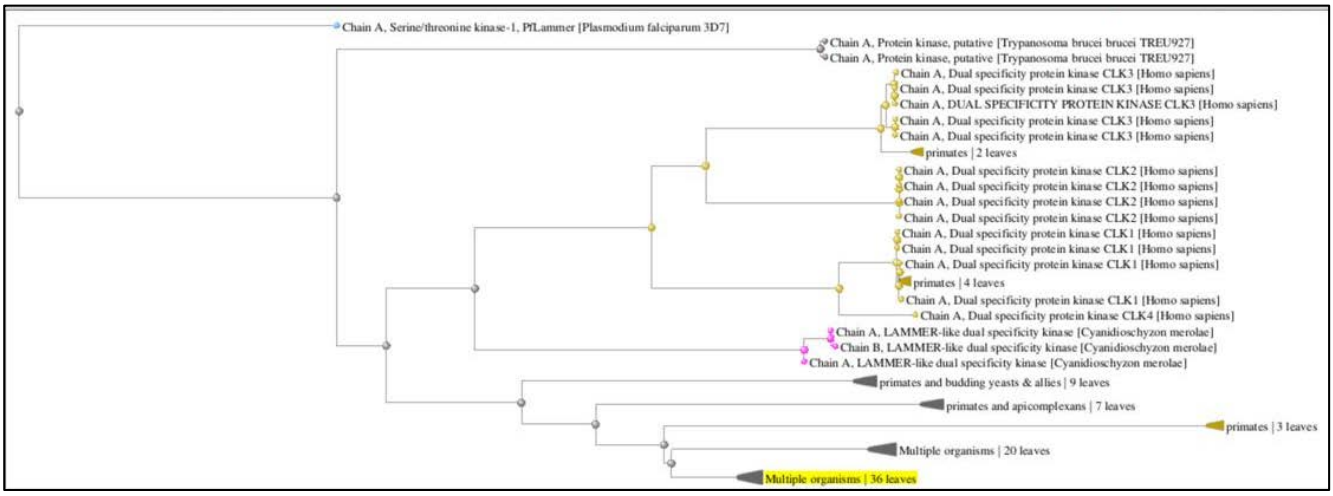

Fig 2: Phylogenetic tree generated with the Fast Minimum Evolution algorithm, showing evolutionary relationships among DYRK1A homologues retrieved from the Protein Data Bank.

3.4 Structural Quality Validation

ERRAT analysis of the DYRK1A structure returned an overall quality factor of 96.37%. Ramachandran plot analysis using PROCHECK showed that 88.7% (539 residues) of the structure fell within the most favoured regions, 10.9% (66 residues) in additionally allowed regions, 0.1% (1 residue) in generously allowed regions, and 0.2% (2 residues) in disallowed regions.[32, 33, 34]

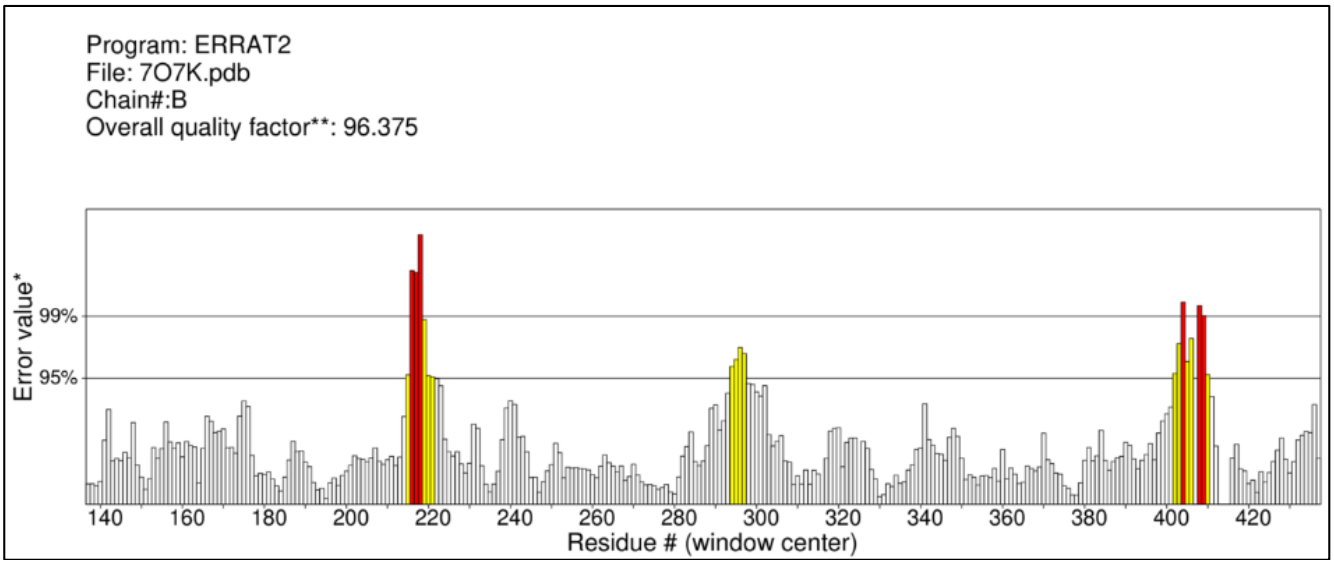

Fig 3: ERRAT validation plots for chain A (top) and chain B (bottom) of human DYRK1A (PDB ID: 7O7K), showing an overall quality factor of 96.37%, indicative of excellent structural quality.

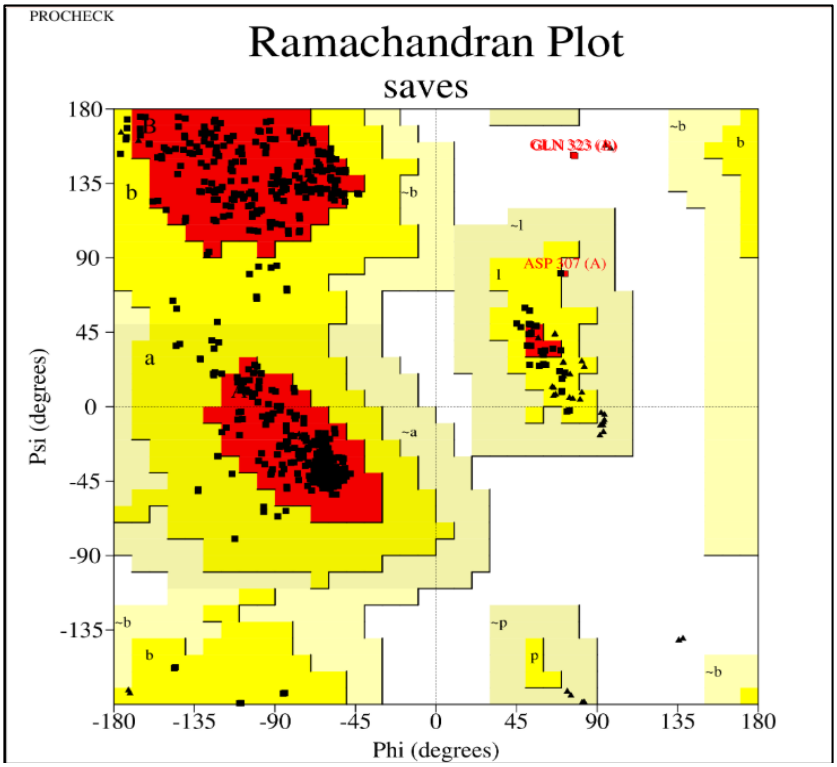

Fig 4: Ramachandran plot of human DYRK1A (PDB ID: 7O7K) generated by PROCHECK, showing 88.7% of residues in the most favoured region and no residues outside the allowed regions other than two isolated outliers.

3.5 B-Factor Analysis

B-factor mapping showed that the majority of the DYRK1A structure exhibited low atomic mobility, consistent with a stable, well-ordered kinase core. Elevated B-factors were largely confined to solvent-exposed loop regions, suggesting localized flexibility that may accommodate conformational adjustment during ligand binding without compromising the overall fold [57].

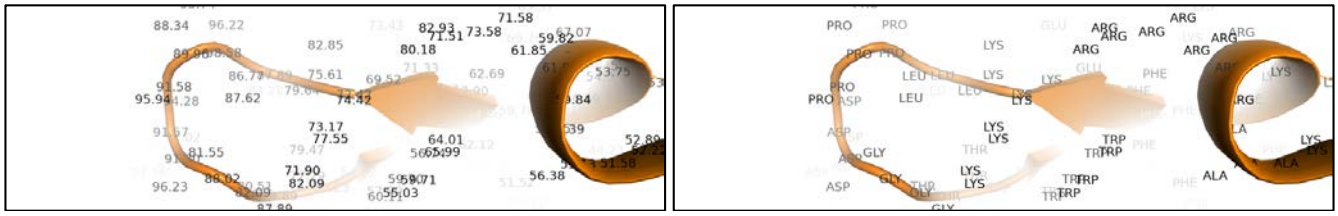

Fig 5: B-factor analysis of human DYRK1A (PDB ID: 7O7K). (A) Structure coloured by B-factor, with blue indicating low atomic mobility and red indicating high atomic mobility. (B) Residue-wise B-factor plots for chains A and B, highlighting solvent-exposed loop regions of elevated flexibility.

3.6 Protein-Protein Interaction Network Analysis

STRING analysis identified DYRK1A as the hub of a ten-partner interaction network comprising DCAF7, RNF169, RAD54L2, LIN52, FAM53C, FAM117B, RCAN1, WDR26, MED13L, and NFATC1. DCAF7 (also known as WDR68), an established binding partner that stabilizes and regulates DYRK1A, showed the highest combined confidence score (0.997). RNF169, RAD54L2, LIN52, FAM53C, and FAM117B, associated with DNA-damage repair, genome stability, and cell-cycle regulation, showed high confidence scores (0.88-0.93), while RCAN1, WDR26, MED13L, and NFATC1, linked to calcineurin-NFAT signalling and transcriptional regulation, showed moderate confidence scores (0.82-0.88) [58, 59].

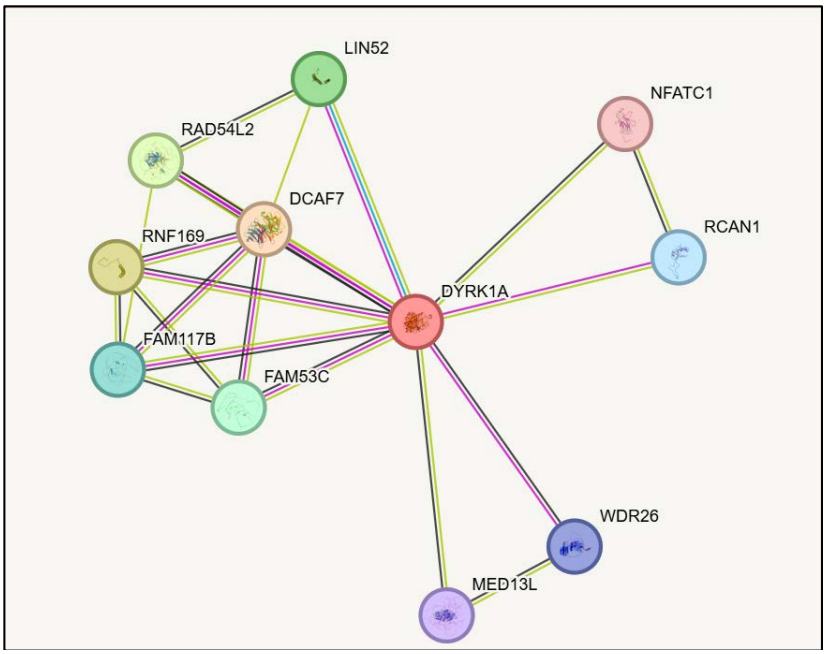

Fig 6: STRING-predicted protein-protein interaction network showing DYRK1A as a central hub, with its ten highest-confidence functional partners spanning

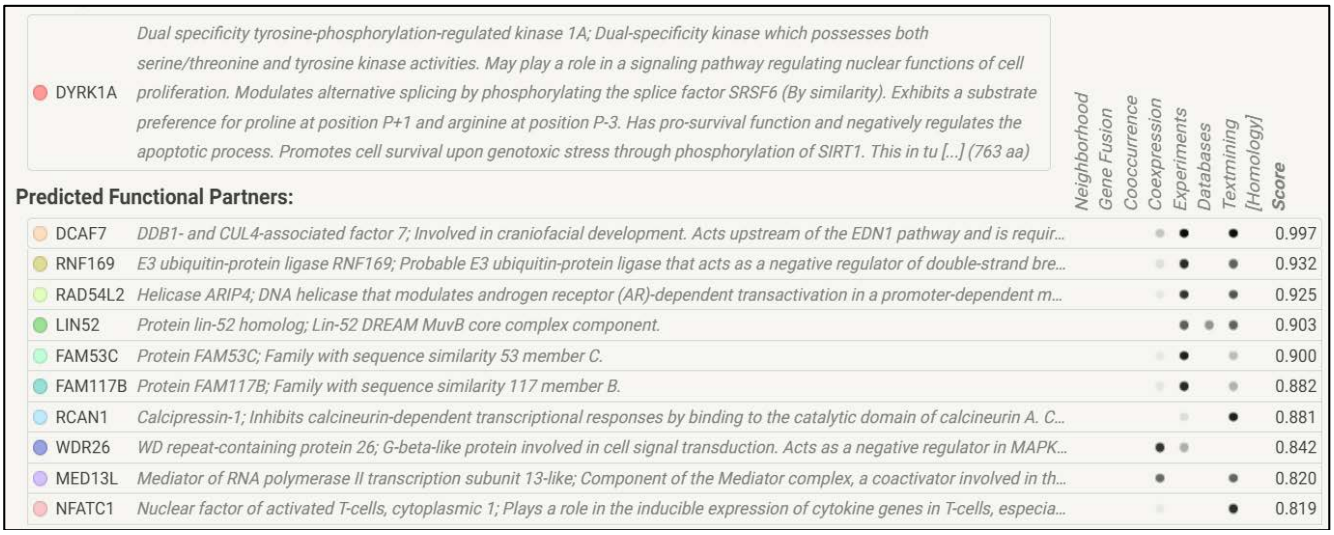

		Neighborhood	Gene Fusion	Cooccurrence	Coexpression	Experiments	Databases	Textmining	[Homology]	Score
DYRK1A	Dual specificity tyrosine-phosphorylation-regulated kinase 1A; Dual-specificity kinase which possesses both serine/threonine and tyrosine kinase activities. May play a role in a signaling pathway regulating nuclear functions of cell proliferation. Modulates alternative splicing by phosphorylating the splice factor SRSF6 (By similarity). Exhibits a substrate preference for proline at position P+1 and arginine at position P-3. Has pro-survival function and negatively regulates the apoptotic process. Promotes cell survival upon genotoxic stress through phosphorylation of SIRT1. This in tu [...] (763 aa)									
Predicted Functional Partners:										
DCAF7	DDB1- and CUL4-associated factor 7; Involved in craniofacial development. Acts upstream of the EDN1 pathway and is requir...									0.997
RNF169	E3 ubiquitin-protein ligase RNF169; Probable E3 ubiquitin-protein ligase that acts as a negative regulator of double-strand bre...									0.932
RAD54L2	Helicase ARIP4; DNA helicase that modulates androgen receptor (AR)-dependent transactivation in a promoter-dependent m...									0.925
LIN52	Protein lin-52 homolog; Lin-52 DREAM MuvB core complex component.									0.903
FAM53C	Protein FAM53C; Family with sequence similarity 53 member C.									0.900
FAM117B	Protein FAM117B; Family with sequence similarity 117 member B.									0.882
RCAN1	Calcipressin-1; Inhibits calcineurin-dependent transcriptional responses by binding to the catalytic domain of calcineurin A. C...									0.881
WDR26	WD repeat-containing protein 26; G-beta-like protein involved in cell signal transduction. Acts as a negative regulator in MAPK...									0.842
MED13L	Mediator of RNA polymerase II transcription subunit 13-like; Component of the Mediator complex, a coactivator involved in th...									0.820
NFATC1	Nuclear factor of activated T-cells, cytoplasmic 1; Plays a role in the inducible expression of cytokine genes in T-cells, especia...									0.819

Fig 7: STRING confidence scores (0.819-0.997) for the ten DYRK1A functional partners

Functional enrichment of this network based on the associated Reference Publications (PubMed) output further supported the involvement of these partners in DNA-damage repair, nuclear transcriptional regulation, chromatin-associated signalling, and neurodevelopmental pathways consistent with the established roles of DYRK1A in neuronal development, synaptic plasticity, and Alzheimer's disease-related pathology.

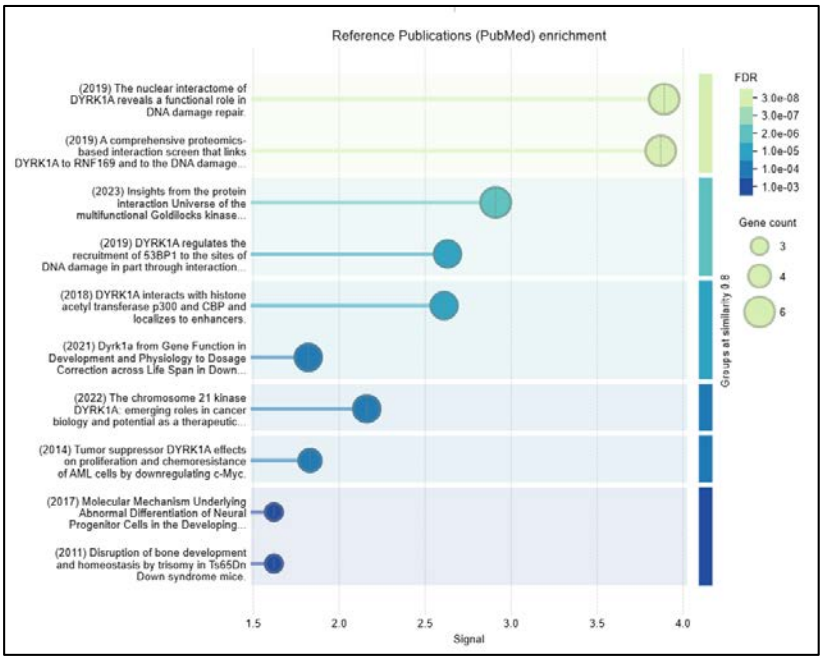

Fig 8: Publications co-citing DYRK1A network members, providing literature-based support for the interaction network

3.7 KEGG Pathway Analysis

Mapping the DYRK1A-centred interaction network onto the KEGG Alzheimer's disease pathway (map hsa05010) placed DYRK1A and its functional partners, including NFATC1, RCAN1, MED13L, WDR26, and DCAF7, within the pathway's amyloidogenic processing, tau-hyperphosphorylation, mitochondrial-dysfunction, oxidative-stress, and neuroinflammatory branches (Figure 10). This convergence between the STRING-derived interaction network and the curated KEGG pathway provides disease-level support for DYRK1A as a therapeutically relevant target and establishes the rationale for the structure-based docking analysis that follows [60, 61].

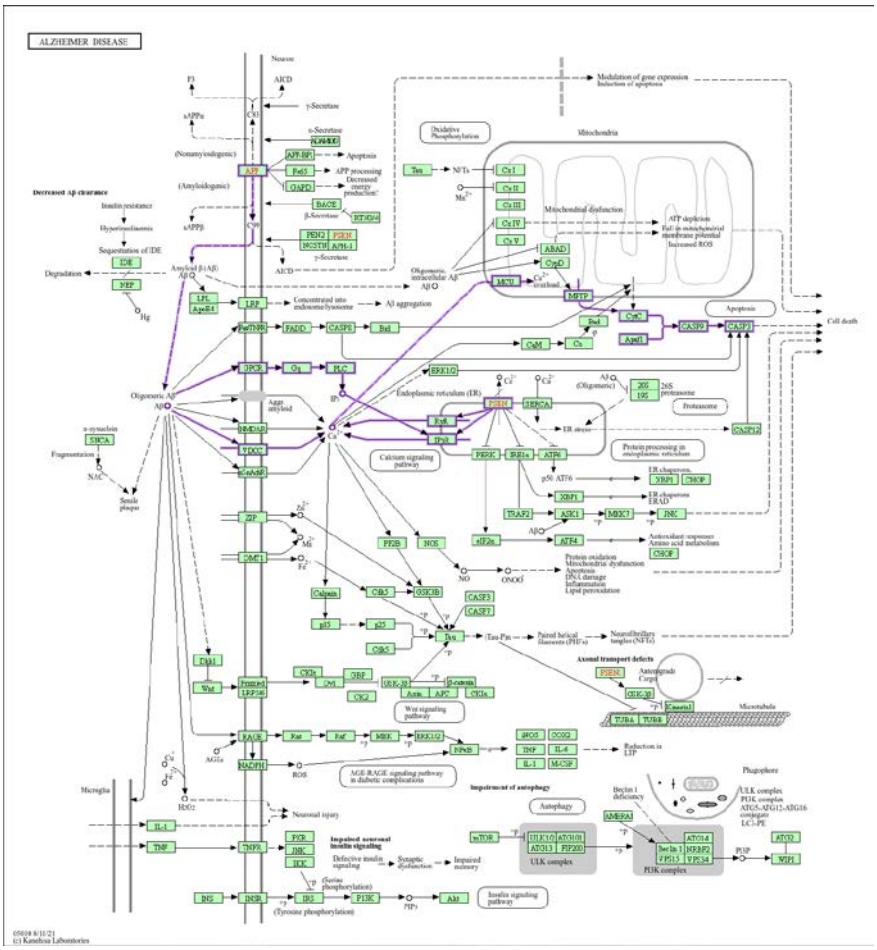

Fig 9: KEGG Pathway Analysis of the DYRK1A-Associated Protein Interaction Network. Mapping of the DYRK1A interaction network onto KEGG

3.8 Molecular Docking

Five candidate ligands, pazopanib, kaempferol, emodin, sunitinib, and the co-crystallized reference inhibitor abemaciclib, were docked against the validated DYRK1A kinase domain using CB-Dock. For each ligand, CB-Dock [62, 63] evaluated five candidate cavities detected by its CurPocket algorithm; the top-ranked cavity for each ligand, identified by its most negative AutoDock Vina score, is summarized in Table 1.

Table 1: Comparative molecular docking analysis of five candidate ligands against the human DYRK1A kinase domain (PDB ID: 7O7K).

PubChem CID	Ligand	Cavity	Vina score (kcal/mol)	Cavity volume (Å³)	Center (x, y, z)	Remarks
10113978	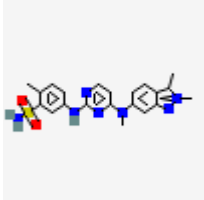 Pazopanib	C1	−10.3	5685	27, −2, 13	Excellent binding
5280863	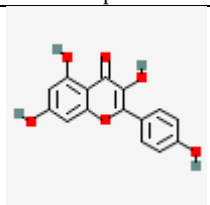 Kaempferol	C2	−8.6	2825	20, 17, 17	Strong binding
3220	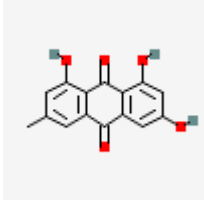 Emodin	C2	−9.2	2825	20, 17, 17	Strong binding
5329102	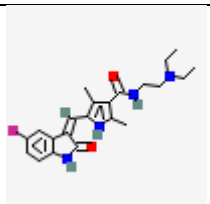 Sunitinib	C1	−8.9	5685	27, −2, 13	Strong binding
46220502	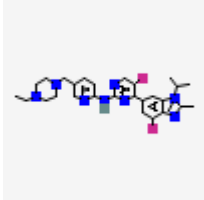 Abemaciclib	C2	−10.7	2825	20, 17, 17	Excellent binding

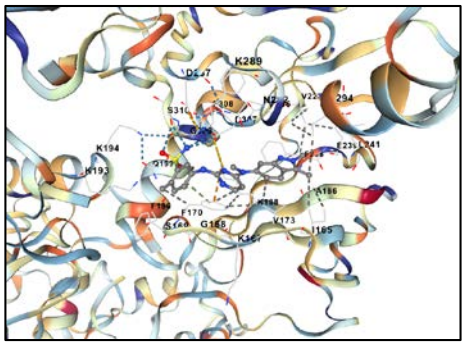

Fig 10: Predicted binding pose and contact-residue analysis of Pazopanib within the DYRK1A ATP-binding cleft (Cavity C1).

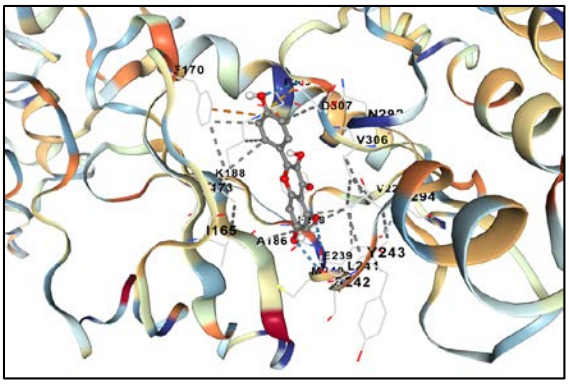

Fig 11: Predicted binding pose and contact-residue analysis of Kaempferol within the DYRK1A

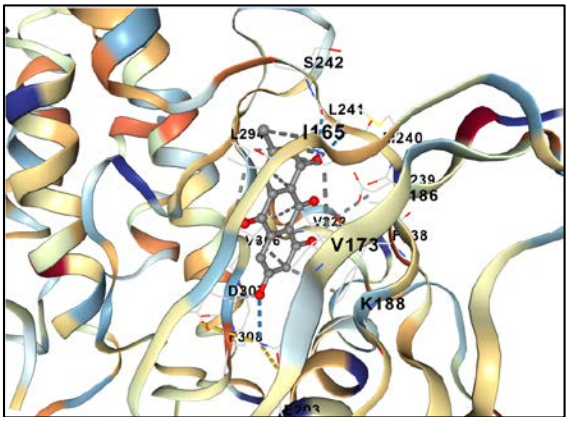

Fig 12: Predicted binding pose and contact-residue analysis of Emodin within the DYRK1A ATP-binding cleft (Cavity C2).

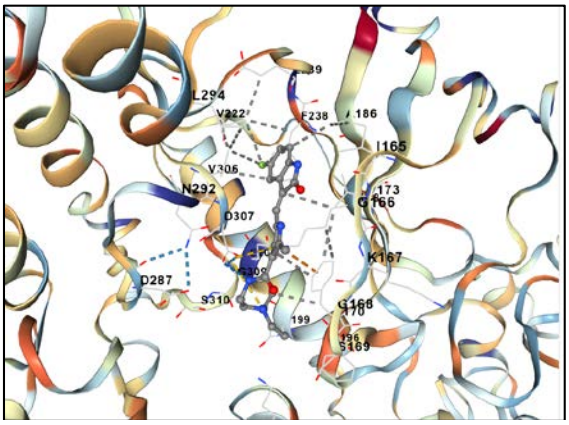

Fig 13: Predicted binding pose and contact-residue analysis of Sunitinib within the DYRK1A ATP-binding cleft (Cavity C1).

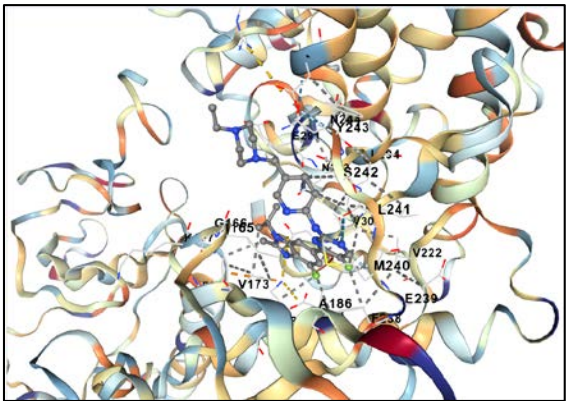

Fig 14: Predicted binding pose and contact-residue analysis of Abemaciclib within the DYRK1A ATP-binding cleft (Cavity C2).

Taken together, all five ligands converged on the same ATP-binding cleft of the DYRK1A kinase domain, sharing a substantially overlapping contact-residue footprint that spans the glycine-rich loop, hinge region, and catalytic loop. Pazopanib and abemaciclib produced the strongest predicted affinities of the panel, while kaempferol, emodin, and sunitinib each showed consistent, favourable engagement of the same pocket.

5. Conclusion

This study retrieved, validated, and structurally characterized the human DYRK1A kinase domain (PDB ID: 7O7K) as a computational template for structure-based drug discovery against Alzheimer's disease. BLASTP and phylogenetic analyses confirmed the identity and evolutionary conservation of the retrieved sequence, [64, 65] while ERRAT and Ramachandran plot analyses confirmed excellent stereochemical quality, and B-factor analysis identified flexible, solvent-exposed loop regions relevant to ligand binding. STRING-based protein-protein interaction analysis placed DYRK1A within a biologically coherent signalling hub linked to DNA-damage repair, calcineurin-NFAT signalling, and transcriptional regulation, and mapping this network onto the KEGG Alzheimer's disease pathway confirmed its involvement in amyloidogenic, tau-hyperphosphorylation, and neuroinflammatory processes central to AD pathology. Building on this validated foundation, CB-Dock-based molecular docking of five candidate ligands identified abemaciclib (−10.7 kcal/mol) and pazopanib (−10.3 kcal/mol) as the strongest predicted binders of the DYRK1A ATP-binding cleft, with kaempferol, emodin, and sunitinib each showing consistent, favourable engagement of the same pocket. Collectively, these findings establish a structurally validated and biologically contextualized basis for advancing this compound panel, particularly pazopanib, toward ADMET profiling and molecular dynamics simulation as part of a drug-repurposing strategy against Alzheimer's disease [66, 67, 68].

References

1. Cummings J, Lee G, Nahed P, Kambar MEZN, Zhong K, Fonseca J, *et al*. Alzheimer's disease drug development pipeline: 2022. Alzheimer's & Dementia (New York, N.Y.). 2022;8(1). doi:10.1002/trc2.12295.
2. Scheltens P, De Strooper B, Kivipelto M, Holstege H, Chételat G, Teunissen CE, *et al*. Alzheimer's disease. Lancet. 2021;397(10284):1577-1590. doi:10.1016/S0140-6736(20)32205-4.
3. Long JM, Holtzman DM. Alzheimer disease: an update on pathobiology and treatment strategies. Cell. 2019;179(2):312-339. doi:10.1016/j.cell.2019.09.001.
4. Wang Y, Mandelkow E. Tau in physiology and pathology. Nature Reviews Neuroscience. 2016;17(1):5-21. doi:10.1038/nrn.2015.1.
5. DeTure MA, Dickson DW. The neuropathological diagnosis of Alzheimer's disease. Molecular Neurodegeneration. 2019;14(1):32. doi:10.1186/s13024-019-0333-5.
6. Goedert M, Eisenberg DS, Crowther RA. Propagation of tau aggregates and neurodegeneration. Annual Review of Neuroscience. 2017;40:189-210. doi:10.1146/annurev-neuro-072116-031153.

7. Gehlot P, Pathak R, Kumar S, Choudhary NK, Vyas VK. A review on synthetic inhibitors of dual-specific tyrosine phosphorylation-regulated kinase 1A (DYRK1A) for the treatment of Alzheimer's disease (AD). Bioorganic & Medicinal Chemistry. 2024;113:117925. doi:10.1016/j.bmc.2024.117925.
8. Kaltheuner IH, Anand K, Moecking J, Düster R, Wang J, Gray NS, *et al*. Abemaciclib is a potent inhibitor of DYRK1A and HIP kinases involved in transcriptional regulation. Nature Communications. 2021;12(1):6607. doi:10.1038/s41467-021-26935-z.
9. Becker W, Sippl W. Activation, regulation, and inhibition of DYRK1A. The FEBS Journal. 2011;278(2):246-256. doi:10.1111/j.1742-4658.2010.07956.x.
10. Wegiel J, Gong CX, Hwang YW. The role of DYRK1A in neurodegenerative diseases. The FEBS Journal. 2011;278(2):236-245. doi:10.1111/j.1742-4658.2010.07955.x.
11. Lionta E, Spyrou G, Vassilatis DK, Cournia Z. Structure-based virtual screening for drug discovery: principles, applications and recent advances. Current Topics in Medicinal Chemistry. 2014;14(16):1923-1938. doi:10.2174/1568026614666140929124445.
12. Ferreira LG, Dos Santos RN, Oliva G, Andricopulo AD. Molecular docking and structure-based drug design strategies. Molecules. 2015;20(7):13384-13421. doi:10.3390/molecules200713384.
13. Qiu N, Qian C, Guo T, Wang Y, Jin H, Yao M, *et al*. Discovery of a novel chemotype as DYRK1A inhibitors against Alzheimer's disease: computational modeling and biological evaluation. International Journal of Biological Macromolecules. 2024;269(Pt 1):132024. doi:10.1016/j.ijbiomac.2024.132024.
14. Chen H, Gao X, Li X, Yu C, Liu W, Qiu J, *et al*. Discovery of ZJCK-6-46: a potent, selective, and orally available DYRK1A inhibitor for the treatment of Alzheimer's disease. Journal of Medicinal Chemistry. 2024;67(15):12571-12600. doi:10.1021/acs.jmedchem.4c00483.
15. Metzker ML. Sequencing technologies—the next generation. Nature Reviews Genetics. 2010;11(1):31-46. doi:10.1038/nrg2626.
16. Goodwin S, McPherson JD, McCombie WR. Coming of age: ten years of next-generation sequencing technologies. Nature Reviews Genetics. 2016;17(6):333-351. doi:10.1038/nrg.2016.49.
17. Bellenguez C, Küçükali F, Jansen IE, Kleineidam L, Moreno-Grau S, Amin N, *et al*. New insights into the genetic etiology of Alzheimer's disease and related dementias. Nature Genetics. 2022;54(4):412-436. doi:10.1038/s41588-022-01024-z.
18. Wightman DP, Jansen IE, Savage JE, Shadrin AA, Bahrami S, Holland D, *et al*. A genome-wide association study with 1,126,563 individuals identifies new risk loci for Alzheimer's disease. Nature Genetics. 2021;53(9):1276-1282. doi:10.1038/s41588-021-00921-z.
19. Kunkle BW, Grenier-Boley B, Sims R, Bis JC, Damotte V, Naj AC, *et al*. Genetic meta-analysis of diagnosed Alzheimer's disease identifies new risk loci and implicates Aβ, tau, immunity and lipid processing. Nature Genetics. 2019;51(3):414-430. doi:10.1038/s41588-019-0358-2.
20. Jansen IE, Savage JE, Watanabe K, Bryois J, Williams DM, Steinberg S, *et al*. Genome-wide meta-analysis identifies new loci and functional pathways influencing Alzheimer's disease risk. Nature Genetics. 2019;51(3):404-413. doi:10.1038/s41588-018-0311-9.
21. Pagadala NS, Syed K, Tuszynski J. Software for molecular docking: a review. Biophysical Reviews. 2017;9(2):91-102. doi:10.1007/s12551-016-0247-1.
22. Berman HM, Westbrook J, Feng Z, Gilliland G, Bhat TN, Weissig H, *et al*. The Protein Data Bank. Nucleic Acids Research. 2000;28(1):235-242. doi:10.1093/nar/28.1.235.
23. Burley SK, Berman HM, Bhikadiya C, Bi C, Chen L, Di Costanzo L, *et al*. RCSB Protein Data Bank: biological macromolecular structures enabling research and education in fundamental biology, biotechnology and energy. Nucleic Acids Research. 2019;47(D1). doi:10.1093/nar/gky1004.
24. Madej T, Lanczycki CJ, Zhang D, Thiessen PA, Geer RC, Marchler-Bauer A, *et al*. MMDB and VAST + : tracking structural similarities between macromolecular complexes. Nucleic Acids Research. 2014;42(Database issue). doi:10.1093/nar/gkt1208.
25. Marchler-Bauer A, Bryant SH. CD-Search: protein domain annotations on the fly. Nucleic Acids Research. 2004;32(Web Server issue). doi:10.1093/nar/gkh454.
26. Kaltheuner IH, Anand K, Geyer M. Crystal structure of the human DYRK1A kinase domain bound to abemaciclib (PDB ID: 7O7K). Protein Data Bank. 2021. doi:10.2210/pdb7O7K/pdb.
27. Wang Y, Geer LY, Chappey C, Kans JA, Bryant SH. Cn3D: sequence and structure views for Entrez. Trends in Biochemical Sciences. 2000;25(6):300-302. doi:10.1016/S0968-0004(00)01561-9.
28. Altschul SF, Madden TL, Schäffer AA, Zhang J, Zhang Z, Miller W, *et al*. Gapped BLAST and PSI-BLAST: a new generation of protein database search programs. Nucleic Acids Research. 1997;25(17):3389-3402. doi:10.1093/nar/25.17.3389.
29. Camacho C, Coulouris G, Avagyan V, Ma N, Papadopoulos J, Bealer K, *et al*. BLAST + : architecture and applications. BMC Bioinformatics. 2009;10:421. doi:10.1186/1471-2105-10-421.
30. Boratyn GM, Schäffer AA, Agarwala R, Altschul SF, Lipman DJ, Madden TL. Domain enhanced lookup time accelerated BLAST. Biology Direct. 2012;7:12. doi:10.1186/1745-6150-7-12.
31. Desper R, Gascuel O. Fast and accurate phylogeny reconstruction algorithms based on the minimum-evolution principle. Journal of Computational Biology. 2002;9(5):687-705. doi:10.1089/106652702761034136.
32. SAVES v6.0. Structural Analysis and Verification Server. UCLA-DOE Institute for Genomics and Proteomics, University of California, Los Angeles.
33. Colovos C, Yeates TO. Verification of protein structures: patterns of nonbonded atomic interactions. Protein Science. 1993;2(9):1511-1519. doi:10.1002/pro.5560020916.
34. Laskowski RA, MacArthur MW, Moss DS, Thornton JM. PROCHECK: a program to check the stereochemical quality of protein structures. Journal of Applied Crystallography. 1993;26:283-291. doi:10.1107/S0021889892009944.

35. Schrödinger LLC. The PyMOL Molecular Graphics System, Version 3.0. 2024.
36. DeLano WL. The PyMOL Molecular Graphics System. DeLano Scientific; 2002.
37. Radivojac P, Obradovic Z, Smith DK, Zhu G, Vucetic S, Brown CJ, *et al*. Protein flexibility and intrinsic disorder. Protein Science. 2004;13(1):71-80. doi:10.1110/ps.03128904.
38. Szklarczyk D, Kirsch R, Koutrouli M, Nastou K, Mehryary F, Hachilif R, *et al*. The STRING database in 2023: protein-protein association networks and functional enrichment analyses for any sequenced genome of interest. Nucleic Acids Research. 2023;51(D1). doi:10.1093/nar/gkac1000.
39. Guard SE, Poss ZC, Ebmeier CC, Pagratis M, Simpson H, Taatjes DJ, *et al*. The nuclear interactome of DYRK1A reveals a functional role in DNA damage repair. Scientific Reports. 2019;9(1):6539. doi:10.1038/s41598-019-42990-5.
40. Glenewinkel F, Cohen MJ, King CR, Kaspar S, Bamberg-Lemper S, Mymryk JS, *et al*. The adaptor protein DCAF7 mediates the interaction of the adenovirus E1A oncoprotein with the protein kinases DYRK1A and HIPK2. Scientific Reports. 2016;6:28241. doi:10.1038/srep28241.
41. Jung MS, Park JH, Ryu YS, Choi SH, Yoon SH, Kwen MY, *et al*. Regulation of RCAN1 protein activity by Dyrk1A protein-mediated phosphorylation. Journal of Biological Chemistry. 2011;286(46):40401-40412. doi:10.1074/jbc.M111.253971.
42. Liu Y, Grimm M, Dai WT, Hou MC, Xiao ZX, Cao Y. CB-Dock: a web server for cavity detection-guided protein-ligand blind docking. Acta Pharmacologica Sinica. 2020;41(1):138-144. doi:10.1038/s41401-019-0228-6.
43. Liu Y, Yang X, Gan J, Chen S, Xiao Z, Cao Y. CB-Dock2: improved protein-ligand blind docking by integrating cavity detection, docking and homologous template fitting. Nucleic Acids Research. 2022;50(W1). doi:10.1093/nar/gkac394.
44. Trott O, Olson AJ. AutoDock Vina: improving the speed and accuracy of docking with a new scoring function, efficient optimization, and multithreading. Journal of Computational Chemistry. 2010;31(2):455-461. doi:10.1002/jcc.21334.
45. Kim S, Chen J, Cheng T, Gindulyte A, He J, He S, *et al*. PubChem 2023 update. Nucleic Acids Research. 2023;51(D1). doi:10.1093/nar/gkac956.
46. Nejabati HR. Kaempferol as a potential neuroprotector in Alzheimer's disease. Journal of Food Biochemistry. 2022;46(9). doi:10.1111/jfbc.14375.
47. Bangar SP, Chaudhary V, Sharma N, Bansal V, Ozogul F, Lorenzo JM. Kaempferol: a flavonoid with wider biological activities and its applications. Critical Reviews in Food Science and Nutrition. 2023;63(28):9580-9604. doi:10.1080/10408398.2022.2067121.
48. Sonpavde G, Hutson TE. Pazopanib: a novel multitargeted tyrosine kinase inhibitor. Current Oncology Reports. 2007;9(2):115-119. doi:10.1007/s11912-007-0007-2.
49. van Geel RMJM, Beijnen JH, Schellens JHM. Concise drug review: pazopanib and axitinib. The Oncologist. 2012;17(8):1081-1089. doi:10.1634/theoncologist.2012-0055.
50. Kanehisa M, Goto S. KEGG: Kyoto Encyclopedia of Genes and Genomes. Nucleic Acids Research. 2000;28(1):27-30. doi:10.1093/nar/28.1.27.
51. Kanehisa M, Furumichi M, Sato Y, Kawashima M, Ishiguro-Watanabe M. KEGG for taxonomy-based analysis of pathways and genomes. Nucleic Acids Research. 2023;51(D1). doi:10.1093/nar/gkac963.
52. Goyal A, Murti Y, Bhushan B, Chisti W, Solanki A. A comprehensive review on therapeutic potential of a natural anthraquinone derivative emodin in brain-related disorders. Current Drug Targets. 2023;24(12):945-958. doi:10.2174/1389450124666230818092506.
53. Faivre S, Demetri G, Sargent W, Raymond E. Molecular basis for sunitinib efficacy and future clinical development. Nature Reviews Drug Discovery. 2007;6(9):734-745. doi:10.1038/nrd2380.
54. Johri V, Kumari U. Sustainable neuroprotection via proteomics and integrative NGS-CADD analysis of 6CVP variant to improve future neurodegenerative health outcomes. IOSR Journal of Pharmacy and Biological Sciences. 2026;21(3):1-10. doi:10.9790/3008-2103010110.
55. Johri V, Kumari U. NGS-based polyglutamine expansion pattern detection using machine learning models to predict the conformation states of Huntingtin. IOSR Journal of Pharmacy and Biological Sciences. 2025;20(5 Ser 3):19-27. doi:10.9790/3008-2005031927.
56. Kumari U, Gunjan, Basak S. NGS contribution in genetic diagnosis for brain disorder. Journal of Clinical Otorhinolaryngology, Head, and Neck Surgery. 2023;27(1):5525-5536.
57. Kumari U, Mukherjee S, Pradhan M, Chakrabarti S. NGS analysis approach for neurodegenerative disease with Biopython. Journal of Emerging Technologies and Innovative Research. 2023;10(9):1-?.
58. Kumari U, Pacholee K. In-silico drug discovery-based approach to treat impairments in patients of Alzheimer's disease. Journal of Emerging Technologies and Innovative Research. 2023;10(12). doi:10.1729/Journal.37001.
59. Kumari U, Gunjan, Basak S. NGS contribution in genetic diagnosis for brain disorder. Journal of Clinical Otorhinolaryngology, Head, and Neck Surgery. 2023;27(1):5525-5536.
60. Nagpal G, Kumari U. Next generation sequence analysis of amyloid precursor-like protein 2 (APLP2) E2 domain in Alzheimer's disease. Journal of Emerging Technologies and Innovative Research. 2025;12(1).
61. Uniyal U, Kumari U. Next generation sequencing data analysis of A25T transthyretin structure associated with Parkinson's disease. Journal of Emerging Technologies and Innovative Research. 2025;12(3). doi:10.1729/Journal.44079.
62. Kokad M, Kumari U. Next-generation sequencing data analysis in DYRK1A associated with neurodegenerative disease. IOSR Journal of Biotechnology and Biochemistry. 2025;11(6):40-48. doi:10.9790/264X-1106014048.
63. Mehrotra K, Kumari U, Pande S. Integrative workflow of Biopython and molecular docking to explore novel

therapeutics targeting PARK7-DJ1. IOSR Journal of Biotechnology and Biochemistry. 2025;11(6):1-10. doi:10.9790/264X-1106010110.
64. Singh N, Kumari U. Multi-omics-based drug discovery pipelines incorporating machine learning, AI, and BioPython in Parkinson's disease: a case study of 5A polymorph of alpha-synuclein. Journal of Emerging Technologies and Innovative Research. 2026;13(2). doi:10.56975/jetir.v13i2.575492.
65. Mandra D, Kumari U, Singh N, Marouthu A. Integrated multi-omics and Biopython approaches for target identification of α-synuclein polymorph in Parkinson's disease. IOSR Journal of Biotechnology and Biochemistry. 2026;12(2):12-21.
66. Singh N, Kumari U, Mandra D, Marouthu A. Integrated machine learning-based toxicity prediction with molecular docking for safer drug candidate screening in Parkinson's disease. Computational Biology and Bioinformatics. 2026;14(1):41-53. doi:10.11648/j.cbb.20261401.14.
67. Johri V, Ramakrishnan S, Tripathi A, Kumari U, Jayaraman A. Structural insights into the interaction of TAP01 antibody with amyloid beta peptide (Aβ pE3-14) for Alzheimer's disease therapeutics. International Journal of Drug Delivery Technology. 2026;16(50s):1007-1017. doi:10.25258/ijddt.16.50s.105.
68. Kumari U, Johri V, Jha T, Dhopate S. Structure-based drug designing for the prediction of epitope for targeting malignant brain tumor. Journal of Emerging Technologies and Innovative Research. 2024;11(7). doi:10.1729/Journal.40433.